Journal of Environmental Radioactivity 177 (2017) 290–304

Contents lists available at ScienceDirect

Journal of Environmental Radioactivity

journal homepage: www.elsevier.com/locate/jenvrad

^{210}Pb and ^{137}Cs as tracers of recent sedimentary processes in two water reservoirs in Cuba

Misael Díaz-Asencio [a, b, *], José Antonio Corcho-Alvarado [c], Héctor Cartas-Aguila [a], Anabell Pulido-Caraballé [a], Carmen Betancourt [d], Joseph M. Smoak [e], Elizabeth Alvarez-Padilla [a], Yeny Labaut-Betancourt [a], Carlos Alonso-Hernández [a], Mabel Seisdedo-Losa [a]

[a] Centro de Estudios Ambientales de Cienfuegos, Carretera Castillo de Jagua km 1.5, Ciudad Nuclear, CP59350, Cienfuegos, Cuba
[b] Instituto de Ecología, Pesquería y Oceanografía del Golfo de México (EPOMEX), Universidad Autónoma de Campeche, Mexico
[c] Spiez Laboratory, Federal Office for Civil Protection, CH-3700 Spiez, Switzerland
[d] University of Cienfuegos "Carlos Rafael Rodríguez", Carretera a Rodas km 3, Cienfuegos, Cuba
[e] University of South Florida, 140 7th Avenue South, St. Petersburg, FL 33701, USA

ARTICLE INFO

Article history:
Received 2 February 2017
Received in revised form
31 May 2017
Accepted 4 July 2017
Available online 17 August 2017

ABSTRACT

Hanabanilla and Paso Bonito Reservoirs are the main fresh water sources for about half a million inhabitants in central Cuba. Prior to this investigation precise information about the losses of storage capacity was not available. Sedimentation is the dominant process leading to reduction in water storage capacity. We investigated the sedimentation process in both reservoirs by analyzing environmental radionuclides (e.g. ^{210}Pb, ^{226}Ra and ^{137}Cs) in sediment cores. In the shallow Paso Bonito Reservoir (mean depth of 6.5 m; water volume of 8×10^6 m^3), we estimated a mean mass accumulation rate (MAR) of 0.4 ± 0.1 g cm^{-2}y^{-1} based on ^{210}Pb chronologies. ^{137}Cs was detected in the sediments, but due to the recent construction of this reservoir (1975), it was not possible to use it to validate the ^{210}Pb chronologies. The estimated MAR in this reservoir is higher than the typical values reported in similar shallow fresh water reservoirs worldwide. Our results highlight a significant loss of water storage capacity during the past 30 years. In the deeper and larger Hanabanilla Reservoir (mean depth of 15.5 m; water volume of 292×10^6 m^3), the MAR was investigated in three different sites of the reservoir. The mean MARs based on the ^{210}Pb chronologies varied between 0.15 and 0.24 g cm^{-2}y^{-1}. The MARs calculated based on the ^{137}Cs profiles further validated these values. We show that the sediment accumulation did not change significantly over the last 50 years. A simple empirical mixing and sedimentation model that assumes ^{137}Cs in the water originated from both, direct atmospheric fallout and the catchment area, was applied to interpret the ^{137}Cs depth profiles. The model consistently reproduced the measured ^{137}Cs profiles in the three cores ($R^2 > 0.9$). Mean residence times for ^{137}Cs in the water and in the catchment area of 1 y and 35–50 y, respectively were estimated. The model identified areas where the catchment component was higher, zones with higher erosion in the catchment, and sites where the fallout component was quantitatively recorded in the sediments.

1. Introduction

Reservoirs play a major role in water and energy supply all over the world. Their sustainable management requires comprehensive knowledge of processes occurring within the reservoir and the catchment basin (Haddadchi et al., 2014; Waters et al., 2015). Sedimentation is one of the most important processes that has significant implications for water storage capacity and water quality in reservoirs (Baskaran et al., 2015).

Sediments in reservoirs have two principal sources: first, allochthonous sediments that originate from eroded rocks and others terrestrial materials within the basin; and second, autochthonous sediments that are produced within the reservoir from the

* Corresponding author. Centro de Estudios Ambientales de Cienfuegos, Carretera Castillo de Jagua km 1.5, Ciudad Nuclear, CP59350, Cienfuegos, Cuba.
E-mail address: misaeldiazasencio1971@gmail.com (M. Díaz-Asencio).

http://dx.doi.org/10.1016/j.jenvrad.2017.07.005
0265-931X/

primary production. The second source may be significant in reservoirs that receive high levels of nutrients from populations or others human activities.

Enhanced erosion within the catchment is commonly the origin of increased sedimentation in reservoirs. Dams interrupt the continuity of sediment through river systems converting reservoirs into major sediment traps (Kondolf et al., 2014). The accumulation of sediments within the reservoir impair their functions and reduces storage capacity. Sedimentation has been recognized as the major threat to reservoir productivity and longevity (Baskaran et al., 2015). Poor land use practices within the catchment basin and the expansion of anthropogenic impacts into previously undisturbed areas are the most common causes of accelerated soil erosion (Kondolf et al., 2014). The increase of erosion in the catchment usually increases the particle loading to the reservoir and with it pollutant fluxes (Betancourt et al., 2010; Lamba et al., 2015; Liu et al., 2013).

Radionuclides ^{210}Pb (half-life: 22 y) and ^{137}Cs (half-life: 30 y) are among the most commonly used tracers to determine recent sediment chronologies. The combination of these two radionuclides have proven to be a powerful tool to investigate sediment deposition and erosion patterns in reservoirs, and provide information vital for understanding the impact of sedimentation in the reservoir (Appleby, 2008; Edgington et al., 1991; Robbins and Edgington, 1975). Sediment chronologies have been used to reconstruct erosion processes in the catchment basin and to determine the flux of pollutants and nutrients in reservoirs (Winston et al., 2014; Chillrud et al., 1999; Perry et al., 2005). These radionuclide techniques have been successfully applied in many lake and reservoir systems including tropical reservoirs (Brenner et al., 1998; Carnero-Bravo et al., 2015; Ruiz-Fernández et al., 2005).

Paso Bonito and Hanabanilla Reservoirs are located in the central part of Cuba. These reservoirs are the sources of fresh water for the cities of Cienfuegos and Santa Clara, which total about half a million inhabitants (Betancourt et al., 2009). A hydroelectric power plant with a capacity of 43 MW is located on the Hanabanilla Reservoir. The reservoirs are therefore of strategic importance for the development of the region.

This paper focuses on the determination of the sedimentation rates in two water reservoirs by applying ^{210}Pb geochronology in several sediment cores. The geochronology is validated with measurements of ^{137}Cs profiles. In addition, a simple mixing and sedimentation model was applied to interpret the ^{137}Cs depth profiles in the sediment cores from the Hanabanilla Reservoir. The model is based on the assumption that ^{137}Cs in the water column originated from both direct atmospheric fallout and from within the catchment area.

2. Materials and methods

2.1. Study area

Hanabanilla and Paso Bonito Reservoirs are located in Arimao River basin (Fig. 1). The main characteristics of the two water reservoirs and their catchment basins are given in Table 1.

2.1.1. Paso Bonito reservoir

The Paso Bonito Reservoir is located to the east of Cienfuegos province, in the Hanabanilla River, downstream of the Hanabanilla Reservoir. This reservoir was constructed in 1975 with the main objective of improving the quality of the water flowing out of the Hanabanilla Reservoir, above the water intakes for the cities of Cienfuegos and Santa Clara (Betancourt et al., 2010). The geology of the catchment basin is characterized by the presence of metamorphic rocks, mainly bluish grey marble. The soils are rich in pyrite and copper deposits, and these resources were exploited prior to1950 (Betancourt et al., 2009).

The population in the catchment basin is less than 600 inhabitants. Human activities are limited to local agriculture production of temporal crops (e.g., rice and tobacco) and permanent plantations of mango and orange. However, the agriculture practices have further developed enhancing soil erosive processes (Betancourt et al., 2009). A previous study in Paso Bonito Reservoir revealed that the accumulation of sediments had already reduced the storage volume of water (Laiz and Flores, 2010). The increase of the sedimentation was explained by the steep slope (mainly mountain and premontane areas) and poor soil management within the watershed of Navarro stream. The study showed that sediments may act as a sink and/or source of nutrients and metals.

2.1.2. Hanabanilla Reservoir

Hanabanilla Reservoir is located in the northern part of the Cienfuegos province, near the border with Villa Clara province (see Fig. 1). The reservoir was constructed between 1958 and 1962 by damming the Hanabanilla and Jibacoa Rivers. To connect both water basins, an artificial water channel was constructed. The reservoir is an elongated, narrow and deep lake that follows the path of the original rivers (Sánchez, 2000). Downstream of the dam, waters are incorporated into the Hanabanilla River through an underground tunnel of 6 km length (Laiz, 2009) (Fig. 1). The catchment of the Hanabanilla dam covers an area of 192 km^2 within the Guamuhaya Mountains. This region has a complex geology, with an extensive area of metamorphic and igneous rocks. Soils in the basin are potentially highly erodible and are characterized by low nutrient content, organic matter and predominantly fine sand fraction (Sánchez, 2000). The local climate is highly influenced by the topography of the region and differs significantly from the climate in the rest of the country. For example, high-intensity rainfalls with short durations are typical in this elevated region (Sánchez, 2000). The population in the catchment basin is less than 7000 inhabitants and the human activities are limited to coffee plantations and local agriculture production. Despite the presence of potentially highly erodible soils in the watershed, little is known about the impact of erosion on the sedimentation rate in Hanabanilla Reservoir.

2.2. Sampling, sample preparation and texture analysis

In 2012, a total of six sediment cores were collected in the reservoirs from areas where no known human disturbance has occurred to the sediment record (Fig. 1, Table 2). An UWITEC corer with PVC liner (90 cm length, 8.6 cm inner diameter) was used for collecting the sediments. Two sediment cores were collected in Paso Bonito Reservoir, one near the dam (PB I) and the second (PB II) at the beginning of the reservoir (upstream side). In Hanabanilla Reservoir four cores were collected, one near the dam (Hn I) and the other three from where the principal basins formed near the rivers inflow: Hanabanilla basin (Hn II), Negro basin (Hn III) and Jibacoa basin (Hn IV). Unfortunately, the core taken in the Jibacoa River basin (near to the second dam) was mixed during the sampling.

In order to optimise the number of samples, to define the sectioning thickness in each core, the length of the core and the date of construction of the reservoir were taken into account. The long cores from the Hanabanilla Reservoir (Hn I and Hn III) were cut at 2 cm, the core Hn II was sectioned at 1.5 cm. This guaranteed a mean temporal resolution of the slices from 1 to 3 years in all cores.

Each section was freeze-dried and homogenized. The dry weight of the sediment was used to determine the dry bulk density (DBD) and the mass accumulation depth according to Sanchez-Cabeza and Ruiz-Fernández (2012). Around 5 g were taken to determine

Fig. 1. Study area in the Hanabanilla and Paso Bonito Reservoirs. Sampling sites are indicated.

Table 1
Principal characteristics of the reservoirs.

Reservoirs	Mean Depth (m)	Surface Area (km^2)	Catchment Area (km^2)	Ratio Surf/Catch.	Volume of water (10^6 m^3)	Year of construction
Hanabanilla	15.5	18.8	192	10.2	292	1962
Paso Bonito	6.5	1.3	65	50	8	1975

Table 2
Location of sampling stations and characteristics of the sediments cores.

Reservoir	Station	Sampling date	Location	Water depth	Core length	Thickness of sections
Paso Bonito	PB I	30/10/2012	N22°07′50″; W80°09′07″	10 m	35 cm	1.5 cm
	PB II	30/10/2012	N22°07′49″; W80°09′02″	8 m	33 cm	1.5 cm
Hanabanilla	Hn I	12/04/2012	N22°05′35″; W80°04′00″	29 m	60 cm	2 cm
	Hn II	12/04/2012	N22°03′15″; W80°04′13.5″	9 m	27 cm	1.5 cm
	Hn III	12/04/2012	N22°02′19″; W80°02′06″	10 m	49 cm	2 cm

grain sizes. The percentage of mud (silt + clay, <63 μm) and sand (>63 μm) were determined by the gravimetric analysis (Loring and Rantala, 1992). The content of organic matter for each section was estimated by the loss on ignition method (LOI: 450 °C, for 8 h). The shape of the LOI profile is used to understand the stratification of sediment in the core.

2.3. Radionuclides

^{210}Pb, ^{226}Ra, ^{40}K and ^{137}Cs were analysed by high-resolution gamma spectrometry using a low-background well-type coaxial Germanium detector (CANBERRA, model Eurisys EGPC 100 P15), with an energy resolution of 2.1 keV at 1333 keV). Approximately 6 g of dry sediments were placed in sealed plastic containers and stored for three weeks, in order to allow ^{226}Ra to reach secular equilibrium with its daughter nuclides. ^{210}Pb was analysed at 46.5 keV gamma ray, ^{226}Ra was determined via the 352 keV gamma rays, emitted by its daughter nuclide ^{214}Pb, and ^{137}Cs was determined through its gamma line at 662 keV. The efficiency calibration was performed using a Standard Uranium Ore (IAEA-RGU-1). The replicate analyses of some samples and certified reference materials IAEA-300, IAEA-375, IAEA-444 and IAEA-306 were used as a quality control tools.

2.4. ^{210}Pb sediment dating

Excess ^{210}Pb (^{210}Pb$_{ex}$) in each section was calculated from the difference between ^{210}Pb and supported ^{210}Pb (^{210}Pb$_{ex}$ = ^{210}Pb - ^{210}Pb$_{sup}$). The ^{210}Pb$_{sup}$ was derived from the ^{226}Ra activity in each layer. The mean Mass Accumulation Rate (MAR; g m^{-2} yr^{-1}) in the sediments were determined through the Constant Flux Constant Sedimentation (CFCS) dating model which assumes a constant flux of ^{210}Pb$_{ex}$ and a constant mean MAR within the period analysed (Robbins and Edgington, 1975). Moreover, the Sediment Accumulation Rate (SAR; cm yr^{-1}) was calculated with this model. The SAR may however be affected by the natural compaction of the sediments and/or by potential sampling compaction. The SAR is only used as informative. The CFCS model was applied to interpret the sedimentation process, where monotonic variations of ^{210}Pb$_{ex}$ *versus* mass depth were found.

In sedimentary systems, where the sediment supply may vary in response to climatic or anthropogenic changes, the Constant Flux (CF) model (Appleby and Oldfield, 1978; Sanchez-Cabeza and Ruiz-Fernández, 2012) is preferentially used. The CF model assumes a constant ^{210}Pb$_{ex}$ flux to the sediment surface, while the MAR may vary. To apply this model, it is necessary to know the total ^{210}Pb$_{ex}$ inventory in the sediment core. This is achieved after approximately 150 years of sediment accumulation. As the investigated reservoirs were constructed in the recent years (1962 and 1975), we will have incomplete ^{210}Pb$_{ex}$ inventories in all the sediment cores. The "missing" inventory of ^{210}Pb$_{ex}$ was estimated using the mean MAR (CFCS model) and the ^{210}Pb$_{ex}$ in the bottom of each cores (Appleby, 1998; Sanchez-Cabeza and Ruiz-Fernández, 2012).

2.5. Age validation with ^{137}Cs

In order to better identify the depth horizon containing the ^{137}Cs peak in 1963, a simple model was used to reconstruct ^{137}Cs depth profiles (Fig. 2). The model assumes that ^{137}Cs in the water reservoir is rapidly scavenged to the sediments, but losses by outflow may also occur. Two sources of ^{137}Cs in the water column are considered. The first source of ^{137}Cs is the direct atmospheric deposition from global fallout, which is assumed to be after deposition well-mixed in the fresh water reservoir. The second source of ^{137}Cs in the water column is runoff/erosive transport from the catchment area (output from the catchment, see Fig. 2) (Porto et al., 2011, 2013).

Assuming that the radionuclide distribution in the water reservoir is described by an exponential function (Corcho-Alvarado et al., 2014), then the maximum annual flux of ^{137}Cs originated by direct fallout (first source) that can be transported to the sediment surface ($F_D(t)$, expressed in Bq m^{-2} y^{-1}), can be calculated as follows:

$$F_D(t) = \sum_{x=1952}^{x=2012} \frac{F_{in}(x) \cdot e^{-\frac{(2012-x)}{T}} \cdot e^{-\lambda(2012-x)} \cdot \Delta x}{T}$$

Where: F_{in} is the time-dependent atmospheric ^{137}Cs history (expressed in Bq m^{-2} y^{-1}), *2012* is the sampling year and *1952* the start of the atmospheric nuclear weapon tests. *T* represents the mean residence time in the well mixed reservoir, *x* is the input year, *ë* is the decay constant of the radionuclide and *Äx* is the summation interval (= 1 y). The time dependent atmospheric ^{137}Cs history in the investigated area (F_{in}) was estimated at 1.162 times the atmospheric deposition of ^{90}Sr for Miami, USA. This multiplication factor accounts for *i)* the different atmospheric deposition of ^{137}Cs and ^{90}Sr (HASL, 1977) and *ii)* the latitudinal and rainfall amount effects between Miami and the study site (Alonso Hernández et al., 2004). The atmospheric deposition before 1950 was assumed to be negligible.

It is assumed that the output of ^{137}Cs from the catchment to the water reservoir is described by an exponential function which is defined by the readily available ^{137}Cs in the catchment area and the catchment/reservoir surface area ratio. The maximum annual flux

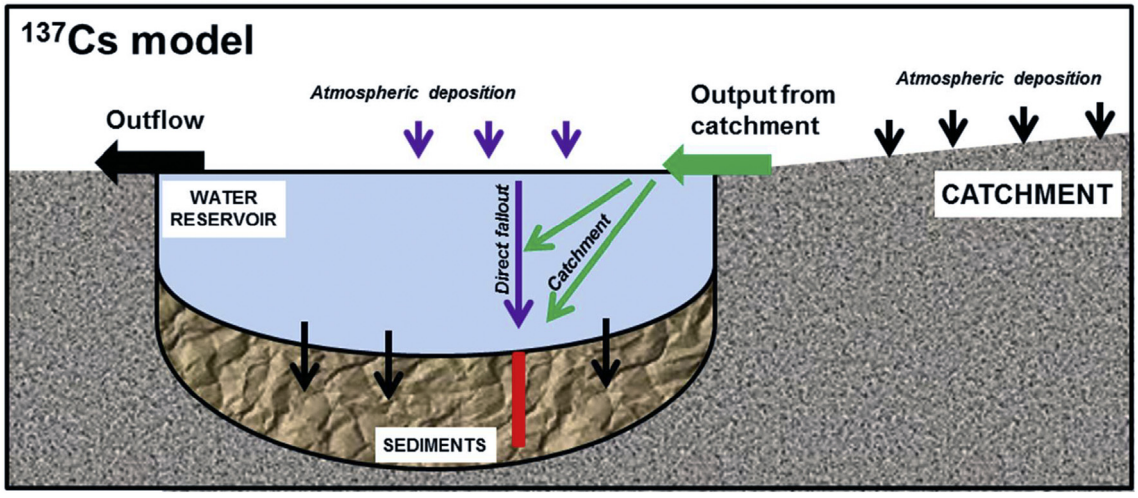

Fig. 2. Representation of the conceptual model used for describing the transport and deposition of ^{137}Cs in the fresh water reservoir. The two main sources of ^{137}Cs in the water column, direct atmospheric fallout and transport from the catchment basin, are represented.

of ^{137}Cs from the catchment area (second source) that can be transported to the sediment surface (F_C *(t)*, expressed in Bq m^{-2} y^{-1}) can be calculated as follows:

$$F_C(t) = \frac{A_c \cdot \gamma}{A_r} \cdot \sum_{x=1952}^{x=2012} \frac{F_{in}(x) \cdot e^{-\frac{(2012-x)}{T}} \cdot e^{-\lambda(2012-x)} \cdot \Delta x}{T}$$

Where: F_{in} is the time-dependent atmospheric ^{137}Cs history (expressed in Bq m^{-2} y^{-1}), *2012* is the sampling year and *1952* the start of the atmospheric nuclear weapon tests. *T* represents the mean residence time in the well mixed reservoir, *x* is the input year, ë is the decay constant of the radionuclide, A_r and A_c are the surface areas of the reservoir and catchment, respectively, Äx is the summation interval (= 1 y) and ã is a parameter that takes into account the fraction of the annual fallout which is readily available for transport. Several studies have shown that ^{137}Cs is strongly fixed to soil particles with long effective half-lives (Corcho-Alvarado et al., 2016; Kinouchi et al., 2015). This fraction can have a large range (i.e., between 7 and 60%) depending on the soils properties, slopes and others (Appleby et al., 2003; Parsons and Foster, 2011; Porto et al., 2013, 2011). It is therefore expected that ^{137}Cs would have a long residence time in the catchment area compared to the scavenging time within the reservoir.

Assuming a constant Mass Accumulation Rate (MAR, kg m^{-2} y^{-1}), the activity of ^{137}Cs ($A_{(i)}$, in Bq kg^{-1}) incorporated into the sediment layer *(i)* can be calculate as:

$$A_i = \frac{(\alpha \cdot F_D(t') + \beta \cdot F_C(t'))}{MAR}$$

Where: á and â are parameters that quantify the fraction of the direct fallout and catchment fluxes (F_D and F_C) that are finally retained in the sediments. Losses from the water column may be expected by outflow transport (Smith et al., 2005). Both parameters are estimated by fitting the modelled data to the measured ^{137}Cs activities.

The ^{137}Cs peak is then associated with the maximum global atmospheric fallout from nuclear testing (1963–1964) and a mean MAR is calculated (Baskaran et al., 2015). The distinct boundary between pre-dam and post-dam sediments may be related to the age of the reservoir and used as an additional time marked to validate the ^{210}Pb$_{ex}$ and ^{137}Cs-based chronologies (Foster et al., 2011; Waters et al., 2015).

3. Results

3.1. Sediment characteristics

The content of fine particles (<63 μm) was above 50% in all depth-sections of the sediment cores collected for this study. In the sediment core from Paso Bonito Reservoir, the fraction of fine particles decreased substantially below 10 cm depth (Fig. 3). In Hanabanilla Reservoir, all cores contained nearly 100% of fine particles (Fig. 4).

The loss of ignition (LOI) was used as an indicator of organic matter content in sediments. In general, the content of OM varied in a narrow range from 10 to 15% in all cores. In the sediment cores from Paso Bonito Reservoir, the LOI showed a significant decrease below 10 cm depth (Fig. 3). In the sediment cores from Hanabanilla Reservoir, the LOI depicted several peaks along the depth profiles (Fig. 4). In the core Hn I, the LOI content was slightly higher than the content in the others cores.

The DBD increased with depth in the two cores of Paso Bonito Reservoir with values higher than 0.4 g cm^{-3} below 10 cm depth. In core PB II, the values were higher than 0.6 below 15 cm (Fig. 3). In the cores of Hanabanilla Reservoir, the DBD increased slightly with depth. In core Hn I, values higher than 0.2 g cm^{-3} were observed only in the 24–25 cm section and in the last four sections of this core. In core Hn II, the values increased with depth after 15 cm; the DBD were higher than 0.4 g cm^{-3} in the last several sections of this core. In core Hn III, the DBD increased slightly with depth, with values higher than 0.2 g cm^{-3} in all sections (except in the surface). The mean DBD in the core Hn I was much lower than the other cores; the high content of water and organic matter in the sediments could be the principal cause of this result (Fig. 4).

3.2. Radionuclides

3.2.1. Paso Bonito reservoir

The ^{210}Pb activities in all the depth-sections of the Paso Bonito cores were below 120 Bq kg^{-1} (Fig. 3). A rather constant activity of ^{210}Pb was observed at the top 10 cm of both cores PB I and PB II (Fig. 3). Below 10 cm depth, the activity of ^{210}Pb decreased. In the core PB II, several peaks were observed in some sections below 15 cm depth. The activities of ^{226}Ra were rather constant in all depth sections of core PB I with values around 40 Bq kg^{-1}. In core PB II a ^{226}Ra constant activity of approximately 45 Bq kg^{-1}was observed in the top 10 cm. Below 10 cm depth, the activities of ^{226}Ra decreased down to a constant value of around 20 Bq kg^{-1}. The secular equilibrium between ^{226}Ra and ^{210}Pb was not reached in either of these two sediment cores (Fig. 3). ^{40}K showed the same pattern as ^{226}Ra in both cases, with constant activities at all depth sections of the core PB I (values around 500 Bq kg^{-1}). In the core PB II a constant activity of ^{40}K was observed in the top 8 cm (values around 600 Bq kg^{-1}). Below 8 cm depth, the activities of ^{40}K decreased down to values between 300 and 400 Bq kg^{-1} (Fig. 3).

^{137}Cs was detected in all depth sections of the cores PB I and PB II with a maximum activity of 10 Bq kg^{-1} in core PB I. In both cores, ^{137}Cs activities decreased with depth, reaching a minimum value of approximately 2.1 Bq kg^{-1} in the core PB II. No significant peak of ^{137}Cs was observed in any of these cores (Fig. 3).

3.2.2. Hanabanilla Reservoir

The maximum ^{210}Pb activities in the sediment cores of Hanabanilla Reservoir were found in the surface layers with values above 200 Bq kg^{-1} with the highest value of 300 Bq kg^{-1} in the core Hn II (Fig. 4). In the three sediment cores, the ^{210}Pb activities showed a monotonic decrease with depth. The activities of ^{226}Ra were rather constant in the three cores with values around 50 Bq kg^{-1}. In core Hn I, the ^{226}Ra profile showed two peaks at approximately 25 and 37 cm depth. In core Hn III, the activities of ^{226}Ra were slightly higher in the bottom sections below 30 cm depth. In two of the cores Hn II and Hn III, ^{226}Ra and ^{210}Pb did not reach secular equilibrium. In the core Hn I, secular equilibrium was reached at the bottom sections of the core (Fig. 4). ^{40}K showed the same pattern as ^{226}Ra in all cases, with activities rather constant in the three cores with values around 500 Bq kg^{-1}. In core Hn I, the ^{40}K profile showed two peaks at approximately 25 and 37 cm depth (Fig. 4).

^{137}Cs was detected in all depth sections of the three sediment cores. The depth profiles of this radioisotope had similar patterns in all the cores with increasing trends with depth and a maximum at the bottom part of the cores (Fig. 4). The maximum activity of ^{137}Cs in the cores Hn II and Hn III was around 30 Bq kg^{-1}. In core Hn I, the peak was more pronounced with a maximum activity of approximately 60 Bq kg^{-1}. The ^{137}Cs peaks were found at 50 cm depth in the cores Hn I and Hn III and at 25 cm depth in the core Hn II (Fig. 4). ^{137}Cs sediment profiles depicted the same pattern observed in the ^{137}Cs global fallout for the region (Robbins et al., 2000).

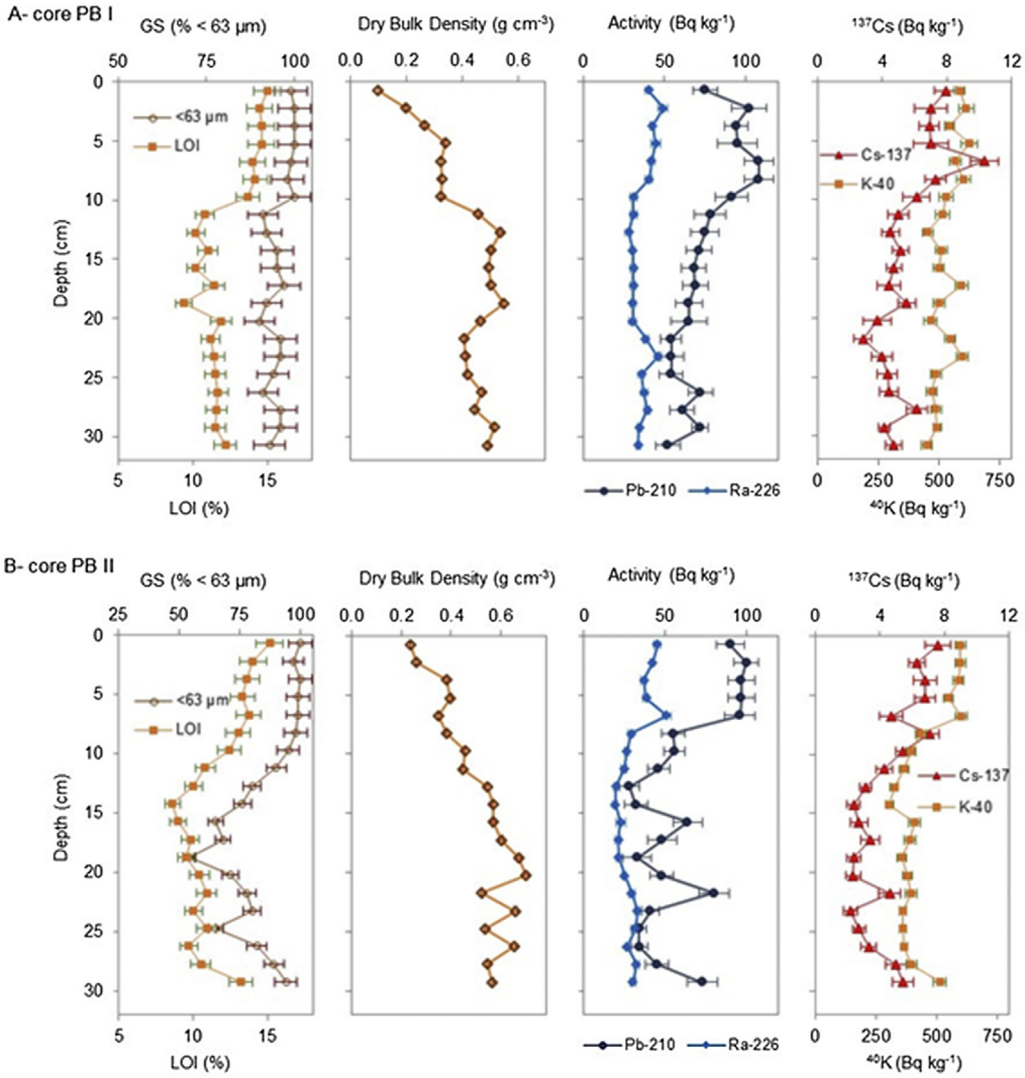

Fig. 3. Vertical profiles of grain sizes, loss of ignition, dry bulk density and radionuclides activities (^{210}Pb, ^{226}Ra, ^{40}K and ^{137}Cs) in two cores of Paso Bonito Reservoir (bars uncertainties = 2σ).

3.3. Sediment geochronology with ^{210}Pb

3.3.1. Paso Bonito reservoir

The ln^{210}Pb$_{ex}$ profiles *versus* mass depth in cores from the Paso Bonito Reservoir are shown in Fig. 5. In core PB I a linear decrease of ln^{210}Pb$_{ex}$ was observed in the upper 20 cm (80 kg m^{-2}) therefore the CFCS model was applied to calculate the accumulation rates in this depth section. This upper section showed an apparent burial rate with a mean MAR of 0.40 ± 0.08 g cm^{-2} y^{-1} in the last 20 years, and a mean sediment accumulation of approximately 1 cm y^{-1}. Below this depth, variable sedimentation was observed. The flux of ^{210}Pb$_{ex}$ in this core estimated with the model CFCS was 247 ± 48 Bq m^{-2} y^{-1}.

Due to the irregular profile of ln^{210}Pb$_{ex}$ in the core PB II the CFCS model was not applicable. However, surface activity of ^{210}Pb in this core was the same as one measured in core PB I, if the flux of ^{210}Pb$_{ex}$ is constant to the reservoir, we then assumed similar MAR in both areas of the reservoir (Appleby, 2008).

3.3.2. Hanabanilla Reservoir

Fig. 6 shows the results of the CFCS ^{210}Pb$_{ex}$ model applied to the sediment cores of Hanabanilla Reservoir. Two distinct burial layers were observed in each core. The mean MAR was nonetheless similar in both layers of each core. The mean MAR was 0.15 ± 0.01 and 0.16 ± 0.02 g cm^{-2} y^{-1} at sites Hn I and II; and 0.24 ± 0.02 g cm^{-2} y^{-1} at site Hn III. The changes observed in the sedimentation process appear to have occurred at the same time (after 1990) in the three cores. The flux of ^{210}Pb$_{ex}$ calculated with the CFCS model was: 233 ± 22 Bq m^{-2}y^{-1} in Hn I, 339 ± 34 Bq m^{-2}y^{-1} in Hn II and 371 ± 30 Bq m^{-2}y^{-1} in Hn III. The mean MAR estimated based on the depth of the ^{137}Cs peak was: 0.16 g cm^{-2}y^{-1} in Hn I; 0.15 g cm^{-2}y^{-1} in Hn II and 0.23 g cm^{-2}y^{-1} in Hn III. These values were nearly identical to those derived via the ^{210}Pb model.

Application of the CF model to the ^{210}Pb data from the Hanabanilla Reservoir cores is shown in Fig. 7A. The "missing" inventory of ^{210}Pb$_{ex}$ was estimated, in each case, before applying the model. The values calculated were of 1675 Bq m^{-2} in core Hn I, 1445 Bq m^{-2} in core Hn II and 1864 Bq m^{-2} in core Hn III. The MARs in the three cores showed a higher variability before 1990, and then after this year remained rather constant. The MARs varied around 0.15 g cm^{-2}y^{-1} in the cores Hn I and Hn II, which were comparable to the mean MAR calculated with the CFCS model. In core Hn I, two significant peaks were observed in the MAR during the years 1977 and 1990. In core Hn III, the MAR increased after 1970 with higher

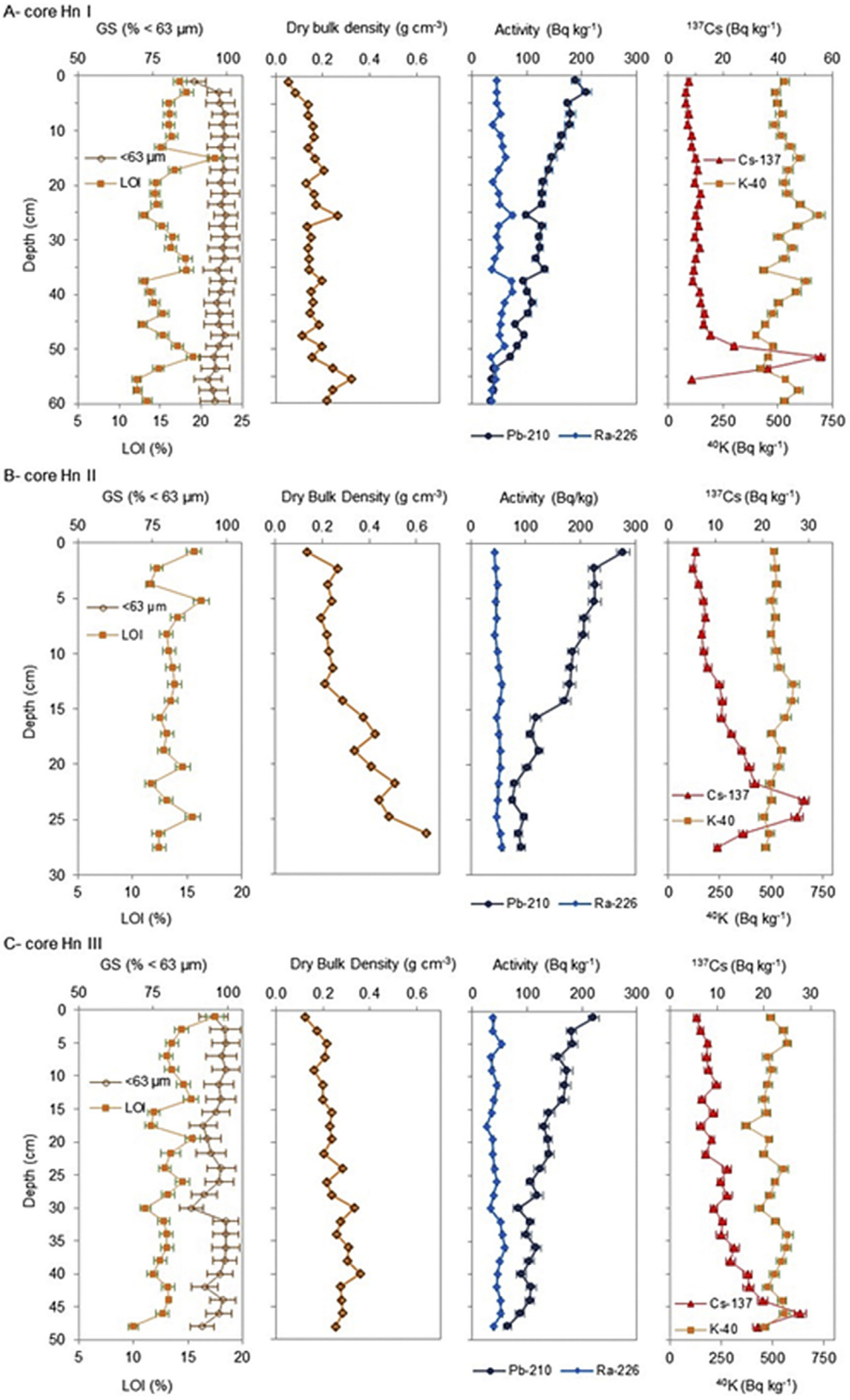

Fig. 4. Vertical profiles of grain sizes, loss of ignition, dry bulk density and radionuclides activities (^{210}Pb, ^{226}Ra, ^{40}K and ^{137}Cs) in three cores of Hanabanilla Reservoir (bars uncertainties = 2σ).

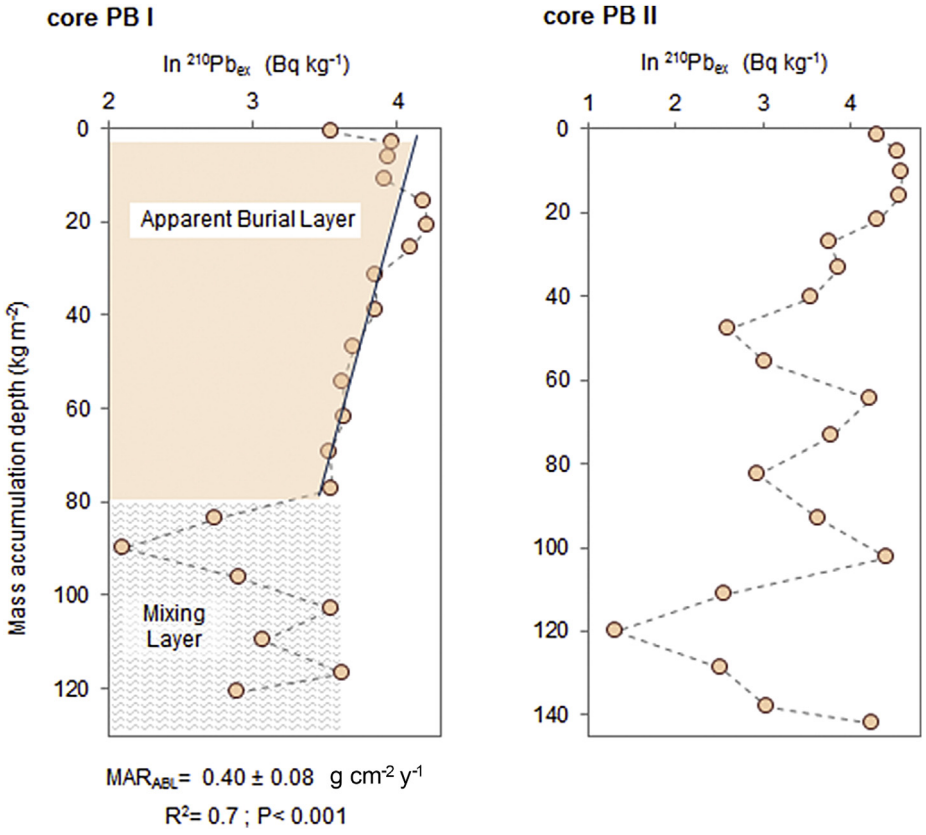

Fig. 5. Vertical profiles of ln $^{210}Pb_{ex}$ in two cores of Paso Bonito Reservoir. Results of the CFCS model in the core PB I.

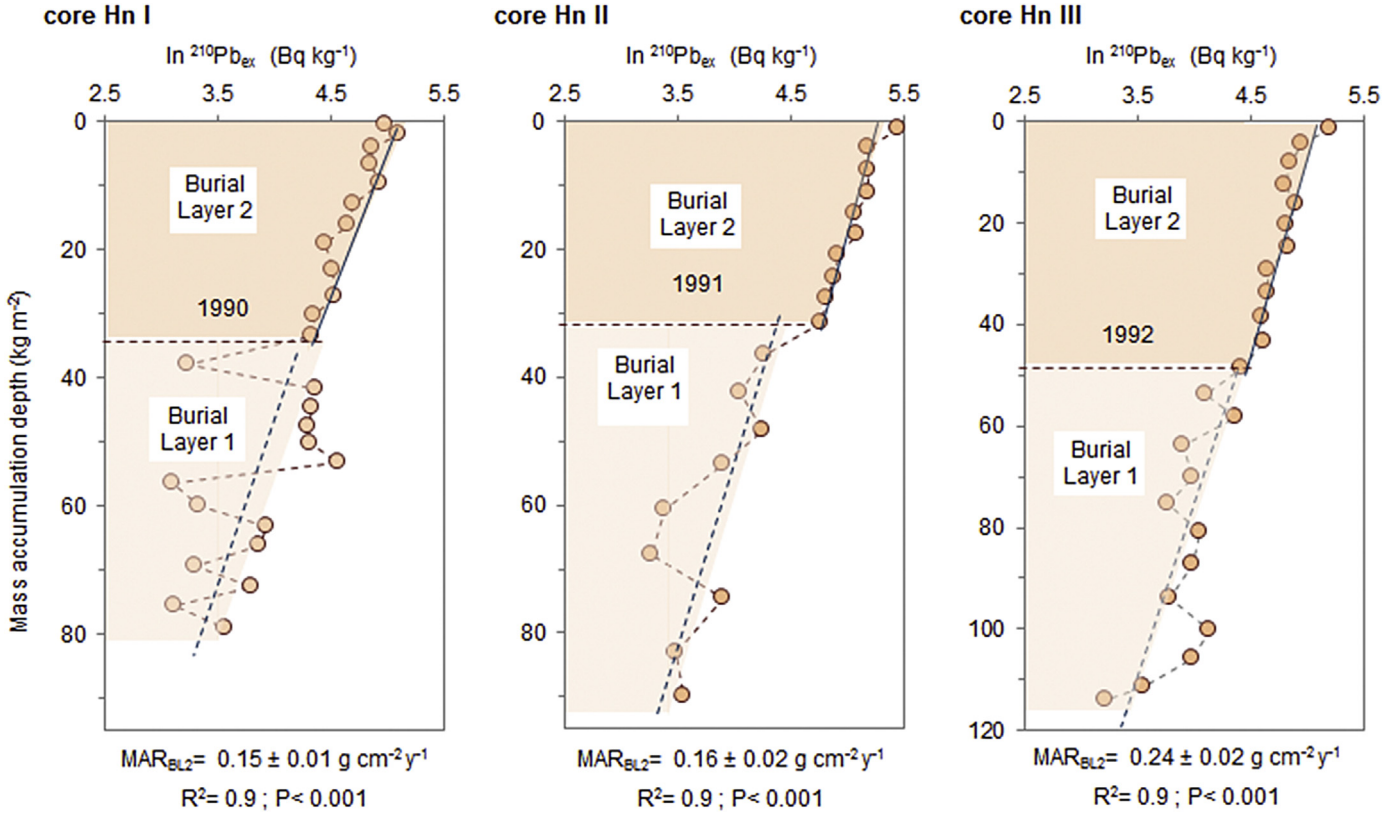

Fig. 6. Vertical profiles of ln $^{210}Pb_{ex}$ in the cores of Hanabanilla Reservoir and results of the CFCS model.

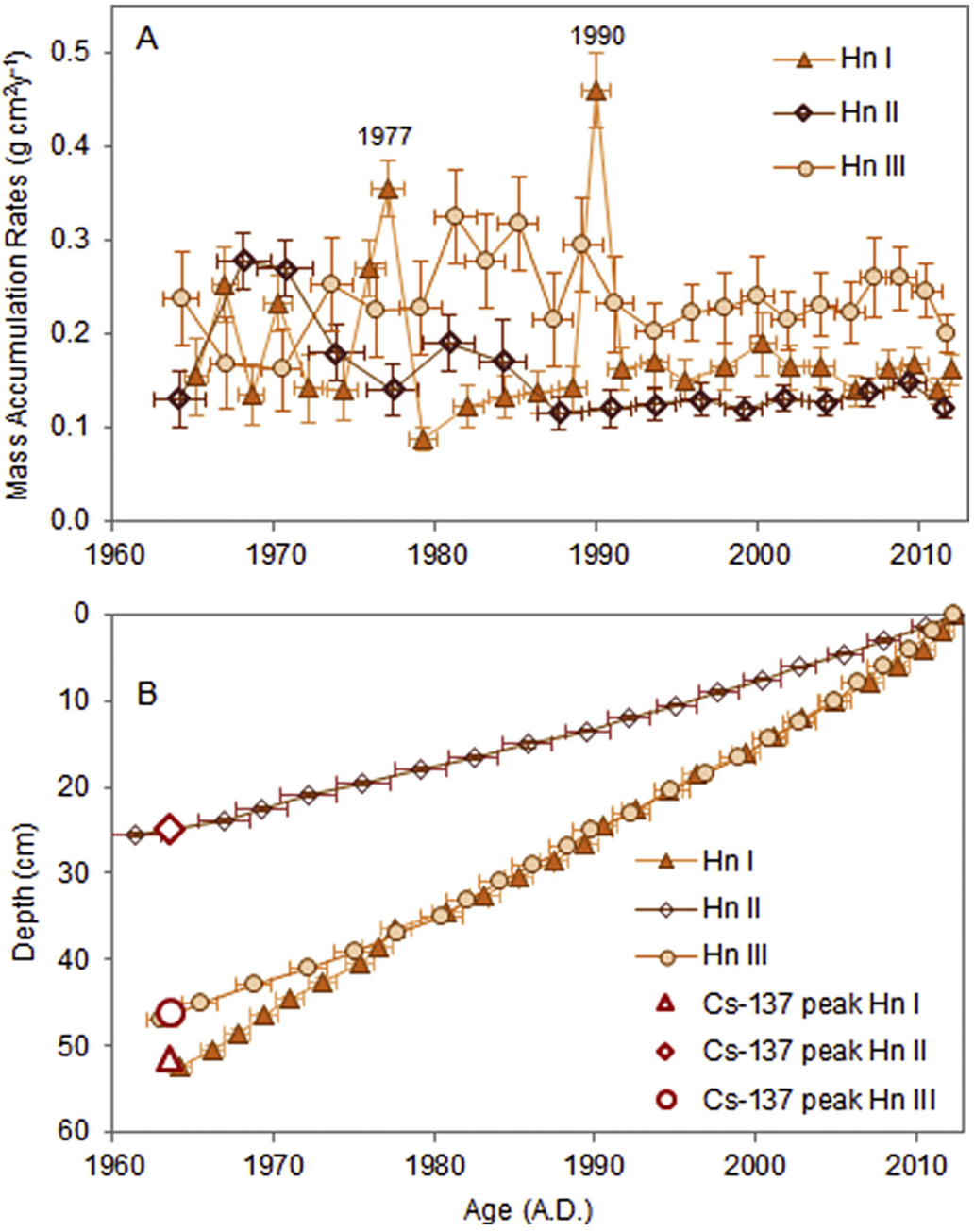

Fig. 7. A) Temporal evolution of the MARs in the cores of Hanabanilla Reservoir, calculated with the CF model. B) Age models with ^{210}Pb and the time marker of peak of ^{137}Cs for each core of Hanabanilla Reservoir (bars uncertainties = σ).

values in the period 1980 to 1990. After 1990, the MAR was stable and comparable to the mean MAR calculated with the CFCS model (0.24 g cm^{-2}y^{-1}). In the three sediment cores, the age derived from the CF model agreed well with age derived from the ^{137}Cs peak (Fig. 7B), assuming that this peak represents the maximum fallout from the nuclear atmospheric weapon tests (Robbins et al., 2000).

The mean sediment accumulation rate (SAR) was 3.1 cm y^{-1} for core Hn I, 0.9 cm y^{-1} for core Hn II and 1.6 cm y^{-1} for core Hn III. From 1963 until 2012, the total sediment accumulation was 52 cm in core Hn I, 25 cm in core Hn II and 49 cm in core Hn III.

4. Discussion

4.1. Sedimentation in the Paso Bonito reservoir

The mean MAR of 0.40 ± 0.08 g cm^{-2} y^{-1} in Paso Bonito Reservoir is higher than the values reported for shallow fresh water reservoirs worldwide. For example, Baskaran et al. (2015) reported mean MAR values from 0.12 to 0.29 g cm^{-2} y^{-1} for the Lake Union; and Waters et al. (2015) estimated values of 0.08–0.30 g cm^{-2} y^{-1} in the Lake Seminole.

The values for the mean MAR obtained in Paso Bonito reservoir were two fold higher than the values calculated for Hanabanilla Reservoir. This is explained by the fact that Paso Bonito Reservoir receives water and sediment particles from three different sources: Hanabanilla Reservoir, Navarro stream and Hanabanilla River. In fact, the Navarro stream is the principal source of suspended particles in this reservoir with almost two times the amount compared to the other two sources (Laiz, 2009). The main reason for the high sedimentation is the high erosion rate in the catchment area of this river, probably from agriculture and mining activities, and the different geologic condition with more erodible rocks (Betancourt et al., 2009).

The mean SAR of 1.0 cm y^{-1} obtained with the CFCS ^{210}Pb dating model in Paso Bonito Reservoir is lower than the value of 5.7 cm y^{-1}, estimated by Laiz and Flores (2010) in the same reservoir using bathymetric studies conducted between 1980 and 2009. In our case, compaction of sediments during sampling may partially explain the lower mean SAR value. This is supported by the greater DBD obtained in both cores in the current study. However, the high value of mean MAR confirms a significant loss of water storage capacity during the past 30 years in this freshwater reservoir. Paso Bonito Reservoir was already reported to have one of the highest losses of water storage capacity per year among the fifteen other fresh-water reservoirs in Cuba (Laiz and Flores, 2010).

4.2. Sedimentation in the Hanabanilla Reservoir

In the three bottom sections of the core Hn I (down 55 cm), the sediments are more consolidated and showed a lighter colour than the rest of the cores. Moreover, $^{210}Pb_{ex}$ was not detected in these sections. These features are a strong indication that these layers represent pre-dam sediments as has been demonstrated in other studies (Waters et al., 2015).

The mean MAR at sites Hn I and Hn II of the Hanabanilla Reservoir were similar with values of 0.15 and 0.16 g cm^{-2} y^{-1}, respectively. In station Hn III, a higher mean MAR of 0.24 g cm^{-2} y^{-1} was derived from the CFCS ^{210}Pb dating model. In cores Hn II and Hn III, the values of the mean SAR (0.5 cm $y^{-1}$and 1.0 cm y^{-1}, respectively) were related to the mean MAR. However, the mean SAR was 1.1 cm y^{-1} in core Hn I which was greater than the expected based on the MAR. This may be explained by the relatively low DBD of the sediments in this core.

In sediment core Hn I, the MARs was greater circa 1964, 1970, 1977 and had a maximum around 1990. After 1990, the MAR remained nearly constant (Fig. 7A). In September 1966, November 1971 and June 1978 intense rains (between 300 and 500 mm in a single day) were reported in Cienfuegos and Villa Clara provinces (Barcia et al., 2011). In June 1988, the region was affected by one of the most intensive rains in the Caribbean with 867 mm in 24 h and nearly 1000 mm in seven days (Barcia et al., 2011). The higher values of MARs in the core Hn I are very probable related to the intense rain events reported in the region. These type of intense and short events are known to increase erosion in the catchment area, and therefore they increase the particulate loading and sedimentation in the aquatic systems (Alonso-Hernandez et al., 2006; Junge et al., 2004). After this extreme event (June 1988), the sedimentation process returned to lower values and remained steady in the reservoir.

In core Hn II, the MAR had higher values between 1968 and 1970, after this period the rate remained nearly constant (Fig. 7A). The highest sediment accumulation rates observed could be related with the intense rains reported during this period in the region (Barcia et al., 2011). In core Hn III, the MARs did not change substantially in time (Fig. 7A). The variations in MARs in the cores due to the extreme rains were different. These results could be related to the coring location within the reservoir. At station Hn I, located near the outlet of the reservoir, management activities during extreme events change the hydrodynamics within the reservoir due to the movement of water (with high solid suspended mater) to the outlet of the reservoir. Then, after these events more material may have been deposited in this area. However, at sites Hn II and Hn III this effect is less important and significant peaks were observed in core Hn II between 1968 and 1970.

The higher sediment accumulation was observed in the core Hn III; located in the artificial channel that connects the two principal basins of the reservoir (Hanabanilla and Jibacoa Rivers basins). The high accumulation of sediments in this area resulted in a rapid decrease in water depth. As a consequence, the water exchange between the two basins decreased, increasing the resident time of the waters in the Jibacoa basin. These changes could affect the quality of the water stored in this sector of the reservoir.

The MAR calculated with the CFCS ^{210}Pb dating model varied between 0.15 and 0.24 g $cm^{-2}y^{-1}$. This range of MAR is comparable to the values reported in other large and deep freshwater reservoirs worldwide. For example, Carnero-Bravo et al. (2015) reported values in the range from 0.12 to 0.56 g $cm^{-2}y^{-1}$ for the Valle de Bravo reservoir in Mexico; and Winston et al. (2014) reported values from 0.2 to 0.8 g $cm^{-2}y^{-1}$ for the Beaver reservoir in USA.

The mean SAR in the Hanabanilla Reservoir (18.8 km^2) calculated based on the design characteristics of an annual water runoff of 137 $\times$ 10^6 m^3 and a mean particulate load rate in the waters of 252 g m^{-3} was estimated to be of 0.2 g $cm^{-2}y^{-1}$ (IGT, 2008). This MAR value is similar to the values obtained with the ^{210}Pb dating models. These results demonstrate that the original design parameters of this reservoir are still valid, potentially as a consequence of a good management of the reservoir and its catchment. The good agreement further supports the applicability of the ^{210}Pb dating models as a tool to evaluate sedimentation processes in freshwater systems.

4.3. Age validation with ^{137}Cs in the Hanabanilla Reservoir

^{210}Pb accumulation rates in Hanabanilla Reservoir were validated by comparing the ^{210}Pb age-depth profiles with the position of the depth horizon ^{137}Cs peak (1963–1964). A simple empirical mixing and sedimentation model was applied to interpret the ^{137}Cs depth profiles (Fig. 8). The model is based on the assumption that ^{137}Cs in the water column originated from both direct atmospheric fallout and the catchment area. In the models, the mean resident time of 1 yr for the atmospheric fallout and 50 yr for the catchment component (35 yr in the case of Hn II) was used. The modeled ^{137}Cs depth profiles are compared with the measured ^{137}Cs profiles, using the parameters that best fitted the model to the measured data (Fig. 8).

The model predicts the ^{137}Cs components in the sediment cores that originated from direct atmospheric fallout and transported from the catchment area. The catchment component represents the fraction of ^{137}Cs in the catchment basin that is readily available for transport and, on an annual basis, the ^{137}Cs readily available for transport has two main components. Firstly, the freshly deposited ^{137}Cs which we assume that is completely available for transport. Secondly, the ^{137}Cs deposited on previous years, we assume this portion available for transport varies based on soil properties. The second component was estimated to be 20%. This value is in the range reported by other studies (Porto et al., 2011, 2013).

Taking into account a total volume of water of 282 $\times$ 10^6 m^3 and the reported water outflow of 4.3 m^3s^{-1}, a mean residence time for the water in the Hanabanilla Reservoir of 2 years was calculated (IGT, 2008). This mean residence time for the water was similar to the values used for direct atmospheric fallout. The long residence

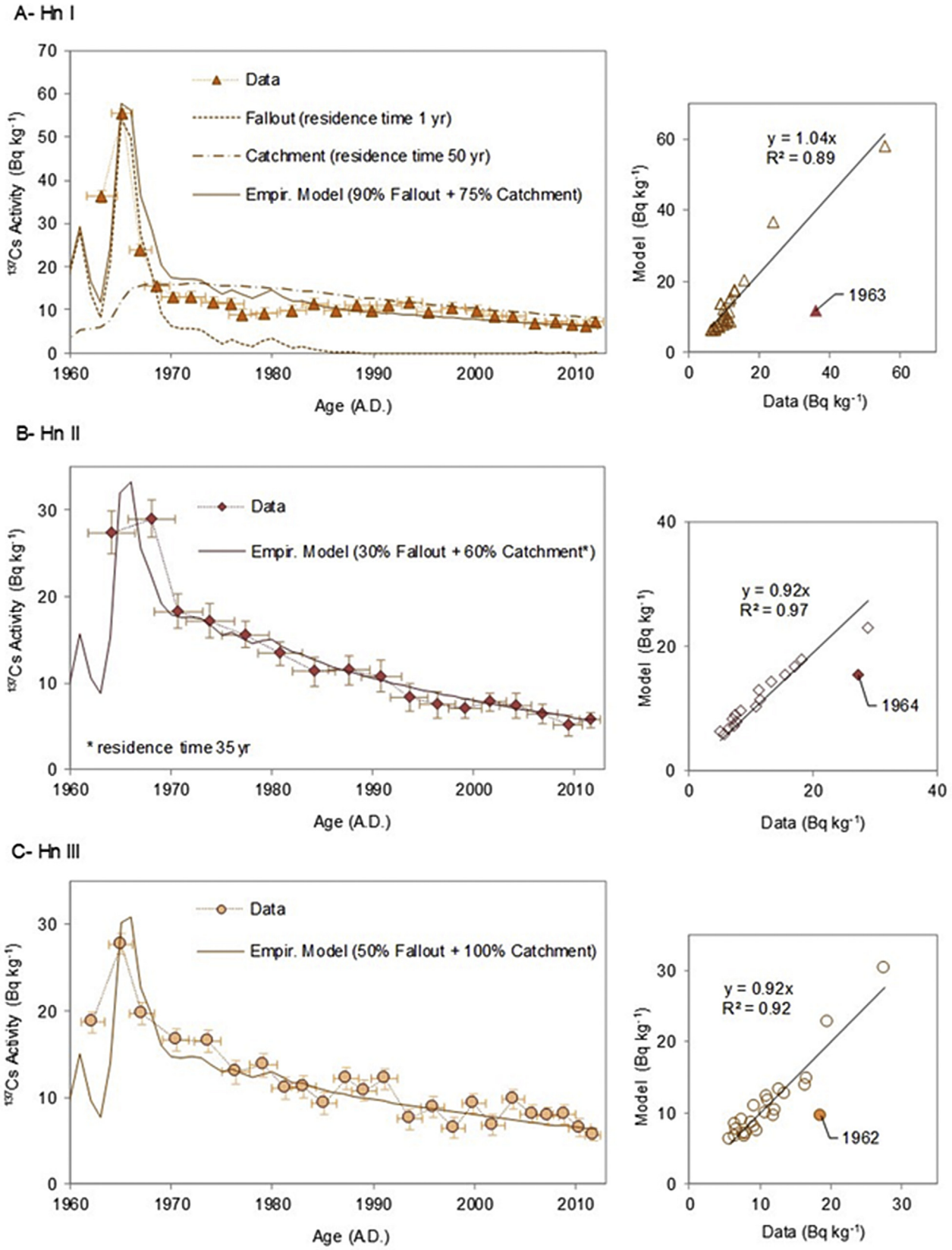

Fig. 8. Models of ^{137}Cs and data in the cores of Hanabanilla Reservoir. Empirical models of ^{137}Cs in the three cores of Hanabanilla Reservoir adjusted for the two sources: atmospheric fallout (resident time 1 yr) and catchment (resident time 50 yr, 35 yr in Hn II). Both component area represented in the core Hn I. The lineal regressions from data vs model are represented in each core.

time of ^{137}Cs in the catchment area (second component) can be explained by its strong adsorption onto some types of soils. Several studies have shown that ^{137}Cs has a long effective half-live in soil (Corcho-Alvarado et al., 2016; Kinouchi et al., 2015).

In the three cores the empirical models reproduced consistently the measured ^{137}Cs depth profiles ($R^2 \geq 0.9$ in the three cores). In Hn I core, the model indicates that sediments in this area captured about 90% of the ^{137}Cs delivered by atmospheric fallout onto the corresponding reservoir surface. Additionally, 75% was delivered by the catchment component. Also the model reproduced the magnitude and location of the depth horizon containing the 1963 fallout maximum.

In core Hn II, the ^{137}Cs fallout component in the sediments represented only 30% of the total atmospheric fallout. In this core the catchment component represented 60% of the total ^{137}Cs that is readily available for transport in the catchment basin. In this case the best fit was obtained using a lower mean residence time of ^{137}Cs in the catchment basin (35 years). This result suggests that ^{137}Cs (as tracer of Cs) in the soils of the Hanabanilla basin is more susceptible to erosion than in soils from other areas (local basins of the cores Hn I and Hn III).

In sediment core Hn III, the ^{137}Cs fallout and catchment components were estimated to be of 50% and 100%, respectively. The model indicates that this area of the reservoir is more affected than the catchment. In fact, this core showed the highest MAR of all the cores in this study, which be explained by a higher particle loading from the catchment basin.

These results showed the principal characteristic of the sedimentation processes in each sampling areas and their drainage basin (Table 3). At site Hn I, the catchment has a lower relative importance on the sediment accumulation than the others areas. On the contrary this component is higher at site Hn III, probably because it receives the influence of the major drainage basin (Jibacoa River). At site Hn II, the local drainage basin (Hanabanilla River) showed a lower mean resident time for ^{137}Cs that the one observed in the others local basin (catchment component). Probably due to the more erodible condition of the soils and consequently, a higher erosion rate in this area compared with other drainage basins of the reservoir.

4.4. $^{210}Pb_{ex}$ flux and ^{137}Cs inventory in the Hanabanilla Reservoir

The total $^{210}Pb_{ex}$ flux in Paso Bonito and Hanabanilla Reservoirs ranged from 233 to 371 Bq m^{-2} y^{-1}. These fluxes are higher than those reported by Binford and Brenner (1986) for Florida lakes (129–204 Bq m^{-2} y^{-1}) and by Brenner et al. (2001) in the Blue Cypress Marsh in Florida (60–125 Bq m^{-2} y^{-1}), USA. Moreover, the $^{210}Pb_{ex}$ flux in Paso Bonito and Hanabanilla Reservoirs are also slightly greater than the flux range reported by Carnero-Bravo et al. (2015) in Valle de Bravo Reservoir (135–199 Bq m^{-2} y^{-1}) in Mexico. The $^{210}Pb_{ex}$ flux range obtained in this study is lower than the ^{210}Pb flux of 577 Bq m^{-2} y^{-1} reported by Baskaran et al. (2015) for the Lake Union Reservoir in USA.

It is generally the case that the total ^{210}Pb supply to lakes and reservoirs is two or three times higher than the direct ^{210}Pb atmospheric input. This is explained by the additional inputs of ^{210}Pb from the catchment area, losses of atmospheric ^{210}Pb from water column via outflow or sediment focusing. Scarce information is available about the atmospheric ^{210}Pb flux in the region where the study sites are located. Alonso-Hernández et al. (2014) reported a relatively low ^{210}Pb flux of 47 Bq m^{-2}y^{-1} in the coastal area of Cienfuegos, a few kilometres south from our studied sites. This low flux was explained by the strong influence of marine winds poorly charged in ^{210}Pb. Considering that our study area is located in a mountainous zone, we expect to have a higher atmospheric ^{210}Pb flux than the one observed in Cienfuegos. The range of $^{210}Pb_{ex}$ fluxes estimated in Paso Bonito and Hanabanilla Reservoirs are not higher than three times the atmospheric ^{210}Pb fluxes and therefore within the limits of application of the CF model. A^{210}Pb supply rate largely deviated from the atmospheric ^{210}Pb flux is one of the main limitations on the use of the CF model for interpreting ^{210}Pb data (Appleby, 2001).

In Fig. 9, the mean MARs in the cores of Paso Bonito and Hanabanilla Reservoirs are plotted against the surface activities of $^{210}Pb_{ex}$ (Hn I is represented but not include in the linear regression). The mean MAR shows a strong negative correlation with the surface activity of $^{210}Pb_{ex}$, which support the application of the CF ^{210}Pb dating model in these cores. The CF model suggest that for sites with a similar atmospheric ^{210}Pb flux, the higher the surface activity of $^{210}Pb_{ex}$ is, the lower the mass accumulation rate (MAR) would be (Appleby, 2001). The site Hn I, did not follow the regression line, possibly due to the lower supply of ^{210}Pb to this site, with values closer to the atmospheric ^{210}Pb flux in the region. This

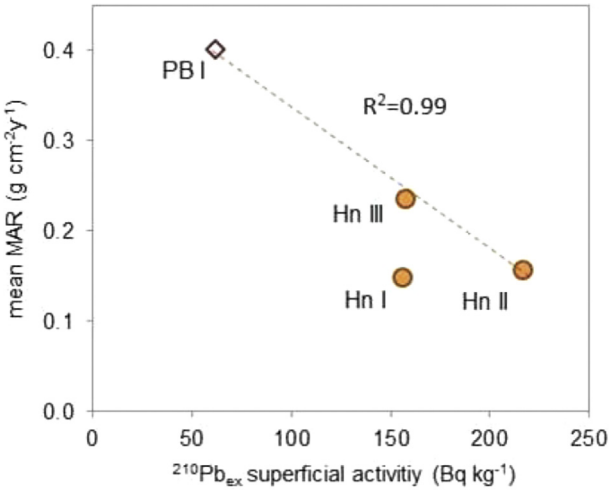

Fig. 9. Linear regression of mean Mass Accumulation Rate *vs.* $^{210}Pb_{ex}$ superficial activities in the cores of Paso Bonito and Hanabanilla reservoir (except core PB II). Hn I is represented but not include in the linear regression.

Table 3
Summary results of the ^{137}Cs and ^{210}Pb models applied in Hanabanilla Reservoir. F and C represent the two sources used in the empirical models of ^{137}Cs (F: Atmospheric Fallout; C: Catchment).

	Sampling site		
	Hn I	Hn II	Hn III
Empirical models of ^{137}Cs profile	90% **F** + 75% **C**	30% **F** + 60% **C**	50% **F** + 100% **C**
^{137}Cs Inventory (Bq m^{-2})	1010	1130	1450
Mean MAR	0.16	0.15	0.23
^{210}Pb Flux	233	339	371

F (residence time 1 yr in all cores); **C** (residence time 50 yr in core Hn I and HnIII; 35 yr in core Hn II).

is explained by a lower input from the catchment area, as was demonstrated with the ^{137}Cs models. Moreover, this site is located near the outflow of the Hanabanilla Reservoir and therefore may have ^{210}Pb losses from water column via outflow.

The inventories of $^{210}Pb_{ex}$ and ^{137}Cs were calculated in the cores from Hanabanilla Reservoir. ^{137}Cs and $^{210}Pb_{ex}$ inventories were calculated by summing the product of each section's activity, thickness and sediment DBD. Due to the recent construction date of the Hanabanilla Reservoir, incomplete inventories of $^{210}Pb_{ex}$ and ^{137}Cs are expected in the sediment cores. The inventories of both radionuclides were calculated for the years from 1963 to 2012. The incomplete inventories of ^{137}Cs in the sediments ranged from 1000 to 1450 Bq m^{-2} (Table 3), the values were in the same range of inventory of ^{137}Cs reported in soils near to Hanabanilla reservoir (Sibello-Hernández et al., 2013).

As discussed previously, the intense rains in 1988 may have caused strong changes in the sedimentation processes in the reservoir. We used this climatic event as a time marker to interpret the changes in the supplies of ^{210}Pb and ^{137}Cs to the sediment cores in two periods; first from 1963 to 1990 and second from 1990 to 2012. The inventories in each stations in the two periods, showed a good linear regression, demonstrating that the ^{210}Pb supply did not change significantly over the past decades at the three stations (Fig. 10A).

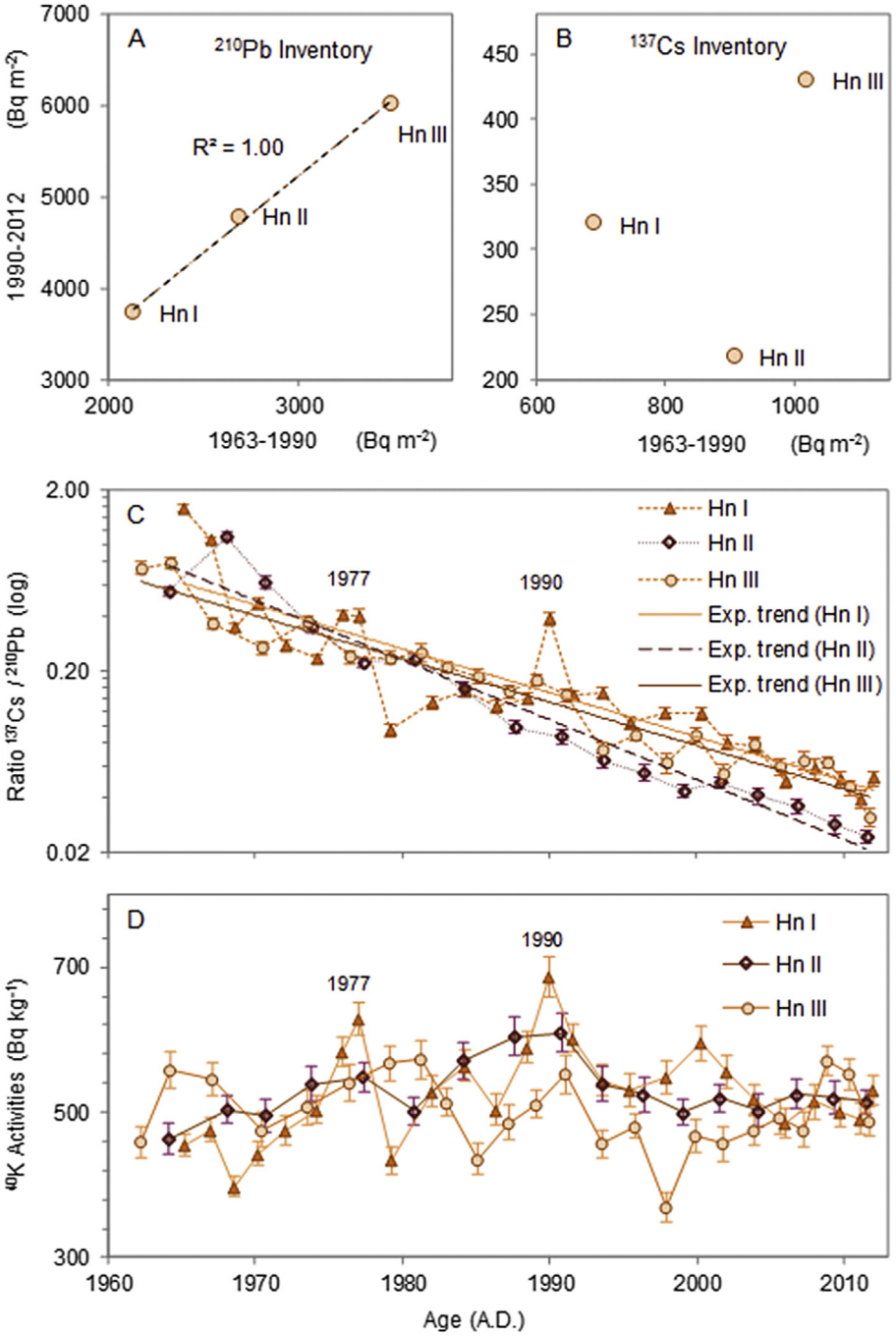

Fig. 10. Ratios of the inventories of ^{210}Pb (A) and ^{137}Cs (B) in the periods 1963–1990 and 1990–2012 in the cores of Hanabanilla Reservoir. C) Ratio of ^{137}Cs/^{210}Pb in time, in these sediment cores. D) Activities of ^{40}K in time in the three cores.

Although the atmospheric fallout of ^{137}Cs has changed significantly in the past 50 years, the ^{137}Cs inventories (1990–2012 *versus* 1963–1990) were similar in cores Hn I and Hn III, however the value expected from 1990 to 2012 was very low in core Hn II (Fig. 10B). This result in core Hn II could be explained by the low levels of ^{137}Cs in the recent sediments by lower fixation as a consequence of more erodible conditions in the local basin, as was observed in Fig. 8. Moreover, in the core Hn II (Fig. 10C) the ratio ^{137}Cs/^{210}Pb$_{ex}$ showed a lower trend after 1980 that the others cores. The relative impoverishment of ^{137}Cs in the more recent sediments in the core Hn II in comparison with the others cores confirm the lower fixation of ^{137}Cs in the sediments, as a results of a more erosion conditions in the local catchment (Hanabanilla River).

The ^{137}Cs/^{210}Pb$_{ex}$ ratio in core Hn I were higher during the intense rains in 1977 and 1988, associated with a change in the material accumulate in this specific slices. This intense rains could produce the re-suspension, transport and accumulation of old soils (with higher ^{137}Cs activities). This justification was used by Alonso-Hernandez et al. (2006), to explain similar patterns observed in sediment cores of the Cienfuegos Bay. Moreover, the value of ^{40}K (associated with mineral composition) in the core Hn I also showed two peaks in 1977 and 1990 (Fig. 10D). This result could be used as confirmation of the change of the sediment composition in these intervals.

5. Conclusions

Sediment chronologies in Paso Bonito and Hanabanilla Reservoirs obtained based on ^{210}Pb data allowed the quantification of sediment accumulation in the systems. Our results confirmed a significant loss of water storage capacity in Paso Bonito Reservoir during the past 30 years. However, the accumulation of sediments in Hanabanilla Reservoir did not change significantly in the past 50 years. This result indicates that current situation of this reservoir still complies with the original design parameters of erosion and sedimentation. Nonetheless, our study identified areas of the reservoir which are more affected by sediment accumulation and by particle loading from the catchment. These results are indeed useful to improve the management of the reservoir and catchment to avoid future problems. The results demonstrated that the geochronology with ^{210}Pb and ^{137}Cs is useful to understand the effect of temporal environmental and human changes on aquatic systems, providing information to improve the management activities.

Acknowledgements

This work was supported by the Nuclear and Advances Technologies Agency (AENTA, Cuba) through the grants PRN 3-1/8-2013 and PNUOLU 4-1-2 2015. We also acknowledge the financial support from the National Council of Science and Technology (CONACYT, Mexico), through the Project CB-2010/153492. We would like to thank the sampling team from the Centre of Environmental Studies of Cienfuegos (CEAC, Cuba): Yurisbey Boza, Lutgardo Vergara, Yudexi Jimenez, Yasser Morera, Jorge Cordoba and Jorge Niebla. We thank to Laura Castellanos (CEAC) for providing the site map. We would like to give thanks to Evelio Utrera in the preparation and analysis of the sediments in CEAC. We also give special thanks to Dr. Jorge M. Garcia Fernandez, Augusto Lopez, Pablo Fuentes and Angel Rodríguez Massip from the National Hydraulic Resources Institute (INRH, Cuba) to help and support the project at all times.

References

Alonso-Hernandez, C.M., Diaz-Asencio, M., Munoz-Caravaca, A., Delfanti, R., Papucci, C., Ferretti, O., Crovato, C., 2006. Recent changes in sedimentation regime in Cienfuegos Bay, Cuba, as inferred from ^{210}Pb and ^{137}Cs vertical profiles. Cont. Shelf Res. 26, 153–167. http://dx.doi.org/10.1016/j.csr.2005.08.026.

Alonso-Hernández, C.M., Morera-Gómez, Y., Cartas-Águila, H., Guillén-Arruebarrena, A., 2014. Atmospheric deposition patterns of ^{210}Pb and ^{7}Be in Cienfuegos, Cuba. J. Environ. Radioact. 138, 149–155. http://dx.doi.org/10.1016/j.jenvrad.2014.08.023.

Alonso Hernández, C., Cartas Águila, H., Díaz Asencio, M., Muñoz Caravaca, A., 2004. Reconstruction of ^{137}Cs signal in Cuba using ^{7}Be as tracer of vertical transport processes in the atmosphere. J. Environ. Radioact. 75, 133–142. http://dx.doi.org/10.1016/j.jenvrad.2003.11.007.

Appleby, P., 2001. Chronostratigraphic techniques in recent sediments. In: Last, W.M., Smol, J.P. (Eds.), Tracking Environmental Change Using Lake Sediments Volume 1: Basin Analysis, Coring, and Chronological Techniques. Kluwer Academic, pp. 171–203.

Appleby, P.G., 2008. Three decades of dating recent sediments by fallout radionuclides: a review. Holocene 18, 83–93. http://dx.doi.org/10.1177/0959683607085598.

Appleby, P.G., 1998. DATING RECENT SEDIMENTS by ^{210} Pb: PROBLEMS and SOLUTIONS. Stuk A-145, pp. 7–24.

Appleby, P.G., Haworth, E.Y., Michel, H., Short, D.B., Laptev, G., Piliposian, G.T., 2003. The transport and mass balance of fallout radionuclides in Blelham Tarn, Cumbria (UK). J. Paleolimnol. 29, 459–473. http://dx.doi.org/10.1023/A:1024437426878.

Appleby, P.G., Oldfield, F., 1978. The calculation of lead-210 dates assuming a constant rate of supply of unsupported 210Pb to the sediment. CATENA 5, 1–8. http://dx.doi.org/10.1016/S0341-8162(78)80002-2.

Barcia, S.S., Orbe, A.G., López, Z.R., Regueira, M.V., Millán, T.J., Ceballo, P.R., Sánchez, B.R., Angulo, R.R., 2011. Variabilidad y Tendencias del Clima en la provincia Cienfuegos, Cuba. Cienfuegos.

Baskaran, M., Miller, C.J., Kumar, A., Andersen, E., Hui, J., Selegean, J.P., Creech, C.T., Barkach, J., 2015. Sediment accumulation rates and sediment dynamics using five different methods in a well-constrained impoundment: case study from Union Lake, Michigan. J. Great Lakes. Res. 41, 607–617. http://dx.doi.org/10.1016/j.jglr.2015.03.013.

Betancourt, C., Jorge, F., Suárez, R., Beutel, M., Gebremariam, S., 2010. Manganese sources and cycling in a tropical eutrophic water supply reservoir, Paso Bonito Reservoir, Cuba. Lake Reserv. Manag. 26, 217–226. http://dx.doi.org/10.1080/07438141.2010.519856.

Betancourt, C., Suárez, R., Toledo, L., 2009. Patrones de distribución temporal de algunas variables físicas y químicas en el embalse Paso Bonito, Cienfuegos, Cuba. Limnetica 28, 23–34.

Binford, M.W., Brenner, M., 1986. Dilution of ^{210}Pb by organic sedimentation in lakes of different trophic states, and application to studies of sediment-water interactions1. Limnol. Oceanogr. 31, 584–595. http://dx.doi.org/10.4319/lo.1986.31.3.0584.

Brenner, M., Keenan, L.W., Miller, S.J., Schelske, C.L., 1998. Spatial and temporal patterns of sediment and nutrient accumulation in shallow lakes of the Upper St. Johns River Basin, Florida. Wetl. Ecol. Manag. 6, 221–240. http://dx.doi.org/10.1023/A:1008408030256.

Brenner, M., Schelske, C.L., Keenan, L.W., 2001. Historical rates of sediment and nutrient accumulation in marshes of the Upper St. Johns River basin, Florida, USA. J. Paleolimnol. 26, 241–257. http://dx.doi.org/10.1023/A:1017578330641.

Carnero-Bravo, V., Merino-Ibarra, M., Ruiz-Fernández, A.C., Sanchez-Cabeza, J.A., Ghaleb, B., 2015. Sedimentary record of water column trophic conditions and sediment carbon fluxes in a tropical water reservoir (Valle de Bravo, Mexico). Environ. Sci. Pollut. Res. 22, 4680–4694. http://dx.doi.org/10.1007/s11356-014-3703-0.

Chillrud, S.N., Bopp, R.F., Simpson, H.J., Ross, J.M., Shuster, E.L., Chaky, D.A., Walsh, D.C., Choy, C.C., Tolley, L.-R., Yarme, A., 1999. Twentieth century atmospheric metal fluxes into central park lake, New York city. Environ. Sci. Technol. 33, 657–662. http://dx.doi.org/10.1021/es9807892.

Corcho-Alvarado, J.A., Balsiger, B., Sahli, H., Astner, M., Byrde, F., Röllin, S., Holzer, R., Mosimann, N., Wüthrich, S., Jakob, A., Burger, M., 2016. Long-term behavior of ^{90}Sr and ^{137}Cs in the environment: case studies in Switzerland. J. Environ. Radioact. 160, 54–63. http://dx.doi.org/10.1016/j.jenvrad.2016.04.027.

Corcho-Alvarado, J.A., Diaz-Asencio, M., Froidevaux, P., Bochud, F., Alonso-Hernández, C.M., Sanchez-Cabeza, J.A., 2014. Dating young Holocene coastal sediments in tropical regions: use of fallout ^{239,240}Pu as alternative chronostratigraphic marker. Quat. Geochronol. 22, 1–10. http://dx.doi.org/10.1016/j.quageo.2014.02.001.

Edgington, D.N., Klump, J.V., Robbins, J.A., Kusner, Y.S., Pampura, V.D., Sandimirov, I.V., 1991. Sedimentation rates, residence times and radionuclide inventories in Lake Baikal from ^{137}Cs and ^{210}Pb in sediment cores. Nature 350, 601–604. http://dx.doi.org/10.1038/350601a0.

Foster, I.D.L., Collins, A.L., Naden, P.S., Sear, D.A., Jones, J.I., Zhang, Y., 2011. The potential for paleolimnology to determine historic sediment delivery to rivers. J. Paleolimnol. 45, 287–306. http://dx.doi.org/10.1007/s10933-011-9498-9.

Haddadchi, A., Nosrati, K., Ahmadi, F., 2014. Differences between the source contribution of bed material and suspended sediments in a mountainous agricultural catchment of western Iran. CATENA 116, 105–113. http://dx.doi.org/

10.1016/j.catena.2013.12.011.
HASL, 1977. Health and Safety Laboratory Environmental Quarterly: Final Tabulation of Monthly 90Sr Fallout Data: 1954-1976 (New York, USA).
IGT, 2008. Estudio de los recursos hídricos en la cuenca del río Arimao. La Habana. Cuba.
Junge, F.W., Jendryschik, K., Morgenstern, P., Treutler, H.C., Zerling, L., 2004. Sediment cores from river dams as flood archives. Stud. Quat. 21, 187–195.
Kinouchi, T., Yoshimura, K., Omata, T., 2015. Modeling radiocesium transport from a river catchment based on a physically-based distributed hydrological and sediment erosion model. J. Environ. Radioact. 139, 407–415. http://dx.doi.org/10.1016/j.jenvrad.2014.07.022.
Kondolf, G.M., Gao, Y., Annandale, G.W., Morris, G., regory, L., Jiang, E., Zhang, J., Yongtao, C., Carling, P., Fu, K., Guo, Q., Hotchkiss, R., Peteuil, C., Sumi, T., Wang, H.-W., Wang, Z., Wei, Z., Wu, B., Wu, C., Yang, C.T., 2014. Sustainable sediment management in reservoirs and regulated rivers: experiences from five continents. Earth's Futur 2, 256–280. http://dx.doi.org/10.1002/2013EF000184.of.
Laiz, O., 2009. ESTUDIOS CAPACIDAD DE ALMACENAJE EN EMBALSES CUBANOS. La Habana. Cuba.
Laiz, O., Flores, E., 2010. Pérdida de la capacidad de almacenaje en embalses cubanos, un efecto de la sedimentación. Storage capacity lost in cuban reservoirs. An effect of sedimentation. Aqua-LAC 2, 12–21.
Lamba, J., Karthikeyan, K.G., Thompson, A.M., 2015. Apportionment of suspended sediment sources in an agricultural watershed using sediment fingerprinting. Geoderma 239–240, 25–33. http://dx.doi.org/10.1016/j.geoderma.2014.09.024.
Liu, Y., Jia, B., Li, X., Wu, J., Meng, P., Hong, W., Zhao, C., 2013. Characteristic of nutrients and evaluation of heavy metal contamination on sediments among Xinpo pond, Nandu river in Hainan province. Nongye Gongcheng Xuebao/Transactions Chin. Soc. Agric. Eng. 29, 213–224. http://dx.doi.org/10.3969/j.issn.1002-6819.2013.03.029.
Loring, D.H., Rantala, R.T.T., 1992. Manual for the geochemical analyses of marine sediments and suspended particulate matter. Earth-Science Rev. 32, 235–283. http://dx.doi.org/10.1016/0012-8252(92)90001-A.
Parsons, A.J., Foster, I.D.L., 2011. What can we learn about soil erosion from the use of ^{137}Cs? Earth-Science Rev. 108, 101–113. http://dx.doi.org/10.1016/j.earscirev.2011.06.004.
Perry, E., Norton, S.A., Kamman, N.C., Lorey, P.M., Driscoll, C.T., 2005. Deconstruction of historic mercury accumulation in lake sediments, northeastern United States. Ecotoxicology 14, 85–99. http://dx.doi.org/10.1007/s10646-004-6261-2.
Porto, P., Walling, D.E., Callegari, G., 2013. Using ^{137}Cs and ^{210}Pb$_{ex}$ measurements to investigate the sediment budget of a small forested catchment in southern Italy. Hydrol. Process 27, 795–806. http://dx.doi.org/10.1002/hyp.9471.
Porto, P., Walling, D.E., Callegari, G., 2011. Using ^{137}Cs measurements to establish catchment sediment budgets and explore scale effects. Hydrol. Process 25, 886–900. http://dx.doi.org/10.1002/hyp.7874.
Robbins, J.A., Edgington, D.N., 1975. Determination of recent sedimentation rates in Lake Michigan using Pb-210 and Cs-137. Geochim. Cosmochim. Acta 39, 285–304. http://dx.doi.org/10.1016/0016-7037(75)90198-2.
Robbins, J. a., Holmes, C., Halley, R., Bothner, M., Shinn, E., Graney, J., Keeler, G., TenBrink, M., Orlandini, K. a., Rudnick, D., 2000. Time-averaged fluxes of lead and fallout radionuclides to sediments in Florida Bay. J. Geophys. Res. Ocean. 105, 28805–28821. http://dx.doi.org/10.1029/1999JC000271.
Ruiz-Fernández, A.C., Páez-Osuna, F., Urrutia-Fucugauchi, J., Preda, M., 2005. ^{210}Pb geochronology of sediment accumulation rates in Mexico City Metropolitan Zone as recorded at Espejo de los Lirios lake sediments. CATENA 61, 31–48. http://dx.doi.org/10.1016/j.catena.2005.01.003.
Sanchez-Cabeza, J.A., Ruiz-Fernández, A.C., 2012. ^{210}Pb sediment radiochronology: an integrated formulation and classification of dating models. Geochim. Cosmochim. Acta 82, 183–200. http://dx.doi.org/10.1016/j.gca.2010.12.024.
Sánchez, R., 2000. Características del agua del embalse Hanabanilla. Santa Clara.
Sibello-Hernández, R.Y., Febles-González, J.M., Toledo-Sibello, Alicia L., Surí-Suárez, R., 2013. Inventario de referencia de ^{137}Cs para estudios de erosión de los suelos en la provincia de Cienfuegos, Cuba. Nucleus 54, 1–7.
Smith, J., Belova, N., Bulgakov, A., Comans, R., Konoplev, A., Kudelsky, A., Madruga, M., Voitsekhovitch, O., Zibold, G., 2005. The "AQUASCOPE" simplified model for predicting 89,90Sr, 131I, and 134,137Cs in surface waters after a large-scale radioactive fallout. Health Phys. 89, 628–644. http://dx.doi.org/10.1097/01.HP.0000176797.66673.b7.
Waters, M.N., Golladay, S.W., Patrick, C.H., Smoak, J.M., Shivers, S.D., 2015. The potential effects of river regulation and watershed land use on sediment characteristics and lake primary producers in a large reservoir. Hydrobiologia 749, 15–30. http://dx.doi.org/10.1007/s10750-014-2142-8.
Winston, B., Hausmann, S., Escobar, J., Kenney, W.F., 2014. A sediment record of trophic state change in an Arkansas (USA) reservoir. J. Paleolimnol. 51, 393–403. http://dx.doi.org/10.1007/s10933-013-9762-2.